Available online at www.sciencedirect.com

ScienceDirect

Solid State Communications 144 (2007) 220–224

solid state communications

www.elsevier.com/locate/ssc

First-principles studies on the electronic and optical properties of $CeCl_3$ and $CeBr_3$

Chenliang Li[a], Biao Wang[a,b,*], Rui Wang[c], Hai Wang[a]

[a] School of Astronautics, Harbin Institute of Technology, Harbin, China
[b] School of Physics Science and Engineering, Sun Yat-sen University, Guangzhou, China
[c] Department of Applied Chemistry, Harbin Institute of Technology, Harbin, China

Received 10 February 2007; received in revised form 9 July 2007; accepted 23 August 2007 by S. Scandolo

---

Abstract

The structural, electronic and optical properties of $CeCl_3$ and $CeBr_3$ crystals are investigated using the density functional theory within generalized gradient approximation (GGA). The calculated lattice parameters are in good agreement with the experimental data. The energy band structures and density of states are obtained. The optical properties of $CeCl_3$ and $CeBr_3$, including the dielectric function, absorption spectra, refractive index, extinction coefficient and reflectivity are all calculated, and the results are compared with the available experimental data.

PACS: 71.15.Mb; 71.20.-b; 74.25.Gz; 78.20.Ci

Keywords: D. Electronic structure; D. Optical properties; D. Dielectric function; E. Density functional theory

---

1. Introduction

Cerium trihalides, as typical rare-earth trihalides scintillator, possess excellent scintillation properties, such as high light output, fast decay time and excellent energy resolution. Therefore, they are widely used in various fields such as high energy physics, positron emission tomography (PET), as well as some chemical processes involved in the nuclear industry [1]. At present, the structural, electronic and optical properties of CeF_3 have been extensively investigated using both experimental and theoretical methods [2–6]. Comparing with the CeF_3 compound, $CeCl_3$ and $CeBr_3$ show preferable optical and scintillation properties, for example a higher light yield (28 000, 68 000 ph/MeV) [9,10]. The electronic structures and absorption spectra of $CeCl_3$ and $CeBr_3$ have been studied by a number of experimental techniques, such as electron-energy-loss spectroscopy (EELS), X-ray photoemission (XPS) and bremsstrahlung isochromat spectroscopy (BIS) [11,12]. Their structures have also been studied using some theoretical methods [5–8]. But to our knowledge, there is no theoretical report about electronic and optical properties of $CeCl_3$ and $CeBr_3$ using the first-principles method. Moreover, exploring the electronic and optical properties of $CeCl_3$ and $CeBr_3$ should have important significance to improve the range of practical applications of cerium trihalides.

In this work, we present a series of first-principles density function theory calculations on the structural, electronic and optical properties of $CeCl_3$ and $CeBr_3$. We investigate the optical properties, including the dielectric function, absorption coefficient, refractive index, extinction coefficient and reflectivity.

2. Computational method

The calculations are performed using the plane-wave pseudopotential method based on density functional theory (DFT). The Perdew–Burke–Ernzerhof (PBE) generalized gradient approximation (GGA) [13] is used for the exchange and correlation correction. The reason is that a number of studies show that the DFT methods based on the GGA scheme can compute accurately the properties of transition

---

[*] Corresponding author at: School of Astronautics, Harbin Institute of Technology, Harbin, China. Tel.: +86 451 86418251; fax: +86 451 86418251.

E-mail address: lichenliang1980@yahoo.com.cn (C. Li).

0038-1098/$ - see front matter © 2007 Elsevier Ltd. All rights reserved.
doi:10.1016/j.ssc.2007.08.040

metals [14–18]. The structural optimizations are conducted using the Broyden–Fletcher–Goldfarb–Shanno minimization (BFGS), modified to take into account the total energy as well as the gradients. The optical properties are then calculated based on the linear response theory. A plane-wave cutoff energy of 450 eV has been employed throughout.

For optical properties calculations, it is important to use a sufficient number of k-points. Meanwhile, the number of empty bands is essential for the accuracy of the calculations. The changes of the optical properties with the number of k-points and empty bands in the optical matrix elements calculation are tested. For the sampling of the Brillouin zone, the electronic structures and optical properties used a $8 \times 8 \times 10$ and $10 \times 10 \times 12$ k-point grid generated according to the Monkhorst–Pack scheme [19], respectively. The number of empty bands is 50.

The optical properties of $CeCl_3$ and $CeBr_3$ are determined by the frequency-dependent dielectric function $\varepsilon(\omega) = \varepsilon_1(\omega) + i\varepsilon_2(\omega)$ that is mainly connected with the electronic structures. The imaginary part $\varepsilon_2(\omega)$ of the dielectric function $\varepsilon(\omega)$ is calculated from the momentum matrix elements between the occupied and unoccupied within selection rules and given by

$$\varepsilon_2 = \frac{2e^2\pi}{\Omega\varepsilon_0}\sum_{k,v,c}\left|\left\langle\psi_k^c\left|\hat{u}\cdot r\right|\psi_k^v\right\rangle\right|^2\delta\left(E_k^c - E_k^c - E\right),$$

where ω is the light frequency, e is the electronic charge. ψ_k^c and ψ_k^v are the conduction and valence band wavefunctions at $\mathbf{k}$, respectively. The real part $\varepsilon_1(\omega)$ of the dielectric function $\varepsilon(\omega)$ can be derived from the imaginary part $\varepsilon_2(\omega)$ using the Kramers–Kronig dispersion equation. All other optical constants on the energy dependence of the absorption spectrum, the refractive index, the extinction coefficient, the energy-loss spectrum, and the reflectivity can be derived from $\varepsilon_1(\omega)$ and $\varepsilon_2(\omega)$ [20].

3. Structure determination

Both $CeCl_3$ and $CeBr_3$ are hexagonal structures with space group $P6_3/m$, where cerium and halide occupy 2a in (1/3, 2/3, 1/4) and 6 h in (0.375, 0.292, 1/4) sites, respectively [21, 22]. The crystal structures are optimized by force and stress minimization. In the process of optimization, all atoms are moved towards their equilibrium positions. The experimental and calculated lattice parameters are summarized in Table 1. For $CeCl_3$ and $CeBr_3$, the values of the lattice constant a are overestimated by 2% and 4% comparing with the experiment results, respectively. At the same time, the values of the lattice constant c are underestimated 2% and 3%, respectively. These deviations are within the admitted range of the errors of the first-principles methods. Thus, our structures are in reasonable agreement with the experiment.

4. Electronic properties

In the following, we calculate the electronic structures of $CeCl_3$ and $CeBr_3$ at their equilibrium structures. For $CeCl_3$, the energy band structure and partial densities of states are shown in Figs. 1 and 2, respectively. The energy band structure is calculated along the way that contains the highest number of high-symmetry points of the Brillouin zone, namely G → A → H → K → G → M → L → H. The zero energy is arbitrarily taken at the Fermi level (dashed line).

Table 1
Crystal structures of $CeCl_3$ and $CeBr_3$

		$a = b$ (Å)	c (Å)	V (Å^3)
$CeCl_3$	Experiment[a]	7.451	4.313	207.367
	Calculation[b]	7.617	4.209	211.511
$CeBr_3$	Experiment[a]	7.936	4.435	241.895
	Calculation[b]	8.265	4.272	252.772

[a] Ref. [21].
[b] This work.

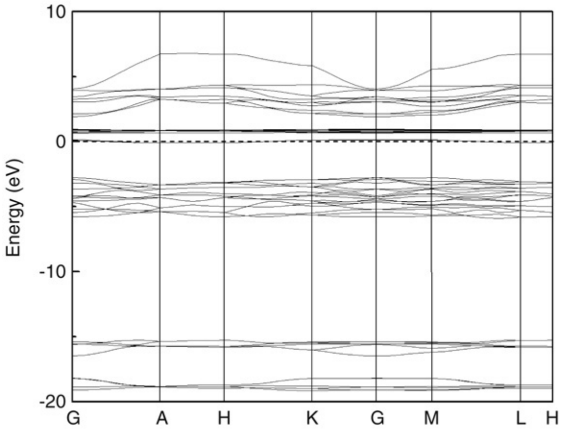

Fig. 1. Band structure of $CeCl_3$ crystal.

The lowest bands around −36 eV consist of 5s states of Ce. The Ce 5p states are located at around −19 eV. The bands around −16 eV are derived from the 3s states of Cl. The energy bands in the range from −6 to −2 eV correspond to the 3p states of Cl that decides the top of the valence band. These results are in agreement with the experimental data [11]. Above the Fermi level, the conduction band consists of 4f and 5d states of Ce. The 4f states have a sharp peak due to its strong localization character. In addition, we found a partly filled f band situated right at the Fermi level. The result does not match the BIS spectrum of $CeCl_3$. This discrepancy may arise from the different treatment method of the 4f states of Ce. If the 4f electron is kept in the core, the calculated result was found to be in agreement with the experimental results [23]. Otherwise, because of the localized character of the f states, the unpaired electron cannot lead to the metallic behavior, its effective mass tending toward infinity [24]. Therefore, $CeCl_3$ is an insulator. Moreover, the $4f^1 \rightarrow 4f^0$ and 4f → 5d calculated energy gap are 0.64 eV and 1.92 eV, respectively. The band gaps predicted by DFT are smaller than experimental data, which means that our results underestimate the real band gaps of $CeCl_3$. In our calculation, the scissors operator (SO) on both the electronic structure and the optical properties are not considered.

The energy band structure and partial density of states of $CeBr_3$ are displayed in Figs. 3 and 4. They are very similar to those of $CeCl_3$ except that the peaks are stronger than those of

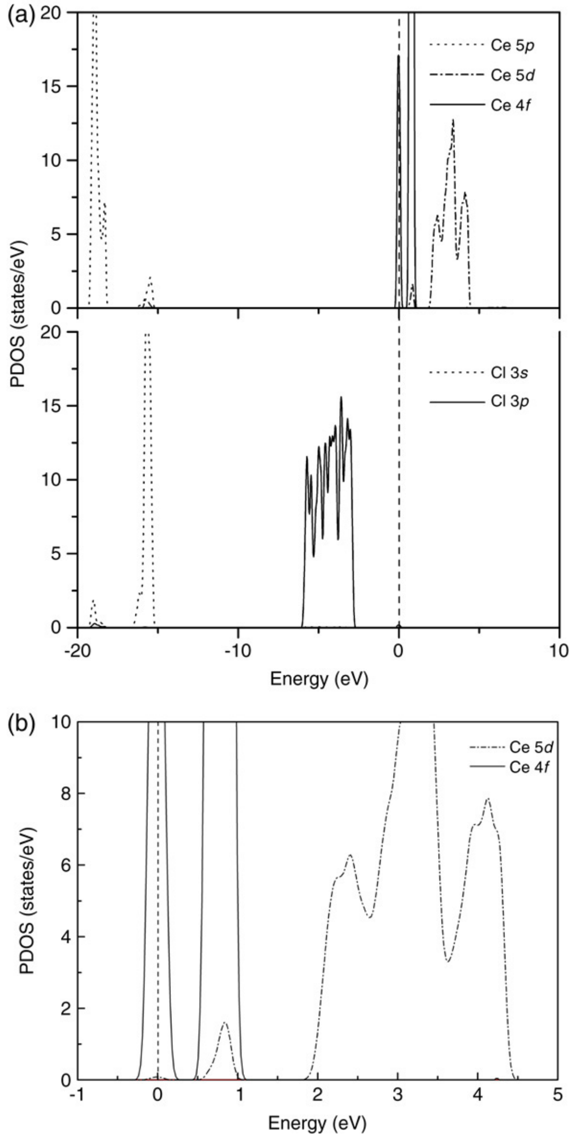

Fig. 2. (a) Partial density of states for $CeCl_3$ crystal; (b) A magnified view of the Ce PDOS around the Fermi level.

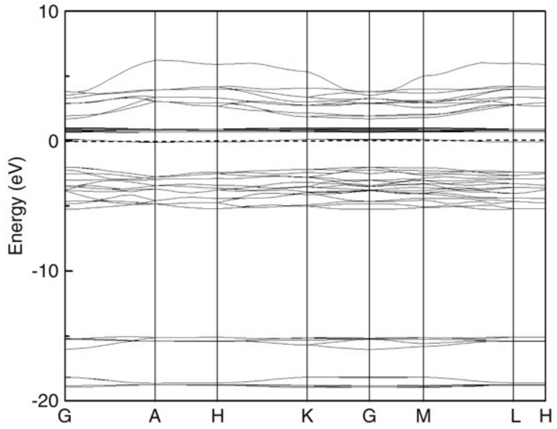

Fig. 3. Band structure of $CeBr_3$ crystal.

$CeCl_3$. It can be seen that the width and the location in energy of the Ce atom are not affected by the halogen ligand Cl/Br.

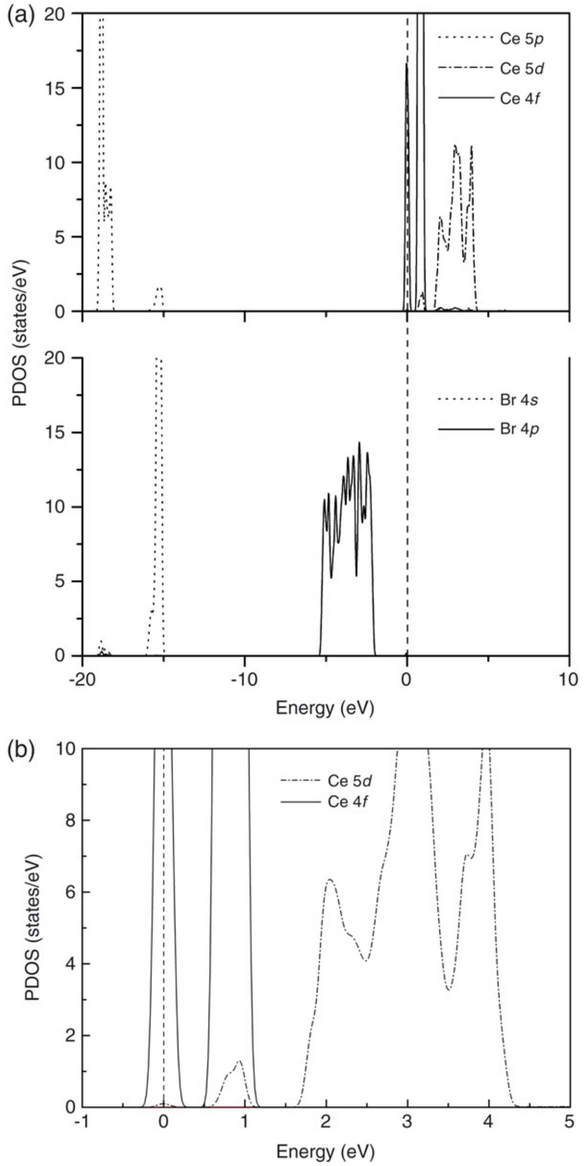

Fig. 4. (a) Partial density of states for $CeBr_3$ crystal; (b) A magnified view of the Ce PDOS around the Fermi level.

5. Optical properties

The dielectric function of $CeCl_3$ is calculated based on its electronic structure. The $\varepsilon_2(\omega)$ and $\varepsilon_1(\omega)$ as a function of the photon energy are shown in Fig. 5. The imaginary part $\varepsilon_2(\omega)$ of the dielectric function is directly connected with the energy band structure. The first peak A at 0.87 eV is due to the transitions from the occupied f states at and just below the Fermi level to the small but finite amount of d states in the sharp fd peak just above the Fermi level. Peak B (3.98 eV) corresponds to the transition $4f^1 \rightarrow 5d^0$ of Ce. The main peaks of C (7.28 eV), D (11.88 eV) and E (12.87 eV) are ascribed to the transition from Cl 3p VB to Ce 5d CB. The peak F (22.17 eV) corresponds mainly to the transition of inner electron excitation from Ce 5p VB to CB. It is noted that a peak in $\varepsilon_2(\omega)$ does not correspond to a single interband transition since many direct or indirect transitions may be found

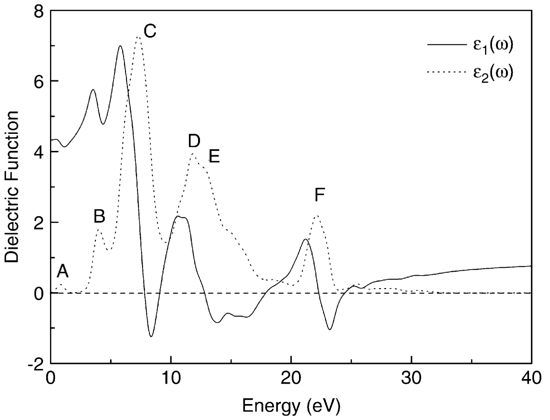

Fig. 5. The imaginary part $\varepsilon_2(\omega)$ and real part $\varepsilon_1(\omega)$ of the dielectric function $\varepsilon(\omega)$ of $CeCl_3$ crystal.

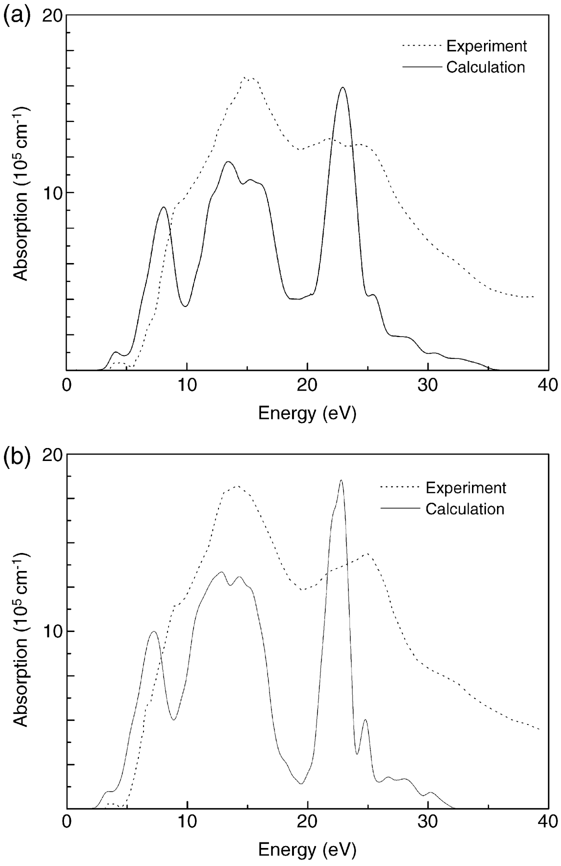

Fig. 6. (a) The absorption spectra of $CeCl_3$; (b) the absorption spectra of $CeBr_3$. The dotted lines represent experimental data and solid lines stand for the calculated result.

in band structure with an energy corresponding to the same peak [25–27].

The absorption spectra of $CeCl_3$ are shown in Fig. 6(a), where the dotted lines represent experimental data and solid lines stand for the calculated result. In the Fig. 7(a)–(c), the solid lines show the calculated results of the refractive index, extinction coefficient and reflectivity of $CeCl_3$, respectively. It is found that the calculated absorption spectrum is in agreement with the experimental data except for at 22.97 eV where the calculated peak value is stronger. This discrepancy could arise from the different treatment method of the 5p states of Ce. According to the experimental result, the absorption peaks at 22.97 and 25.12 eV originate from the transition of $5p_{3/2}$ and $5p_{1/2}$ states of Ce to the lower conduction band. In our calculation, we do not consider the spin–orbit-split for 5p states. The other could be the broadening of the experimental and theoretical curves. The degree of such broadening can influence the intensity of the peak, but it is not given in the experiment. In our calculation, we used Gaussian smearing which is 0.5 eV. However, larger smearing widths result in

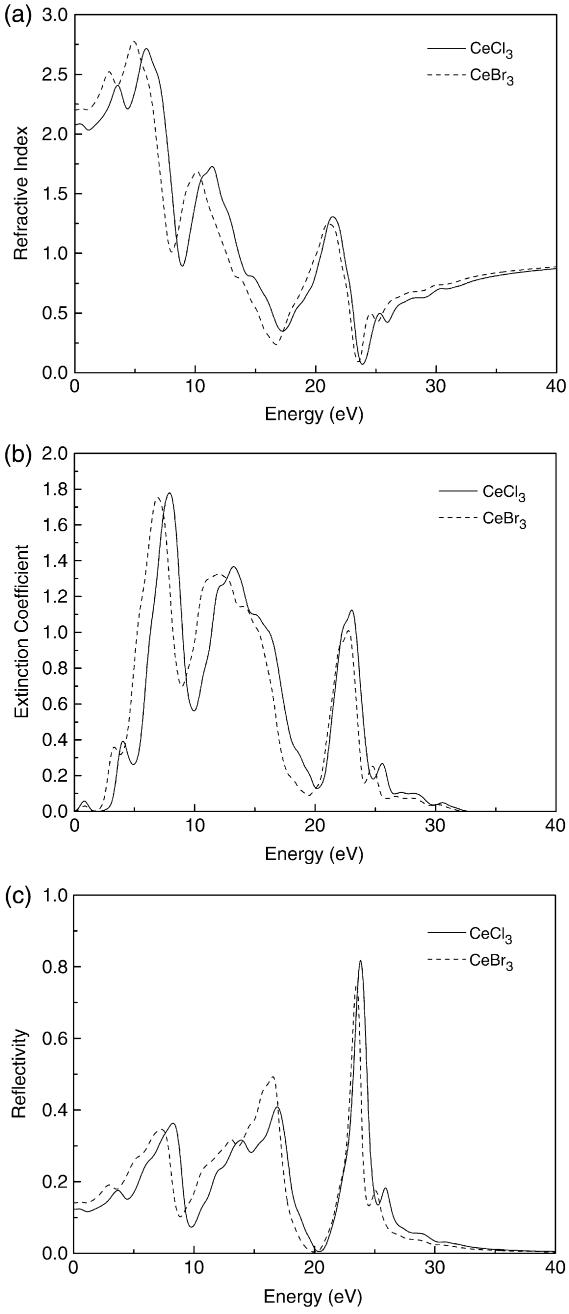

Fig. 7. The calculated optical constants of $CeCl_3$ and $CeBr_3$, (a) refractive index; (b) extinction coefficient and (c) reflectivity. The solid lines and dashed lines stand for $CeCl_3$ and $CeBr_3$, respectively.

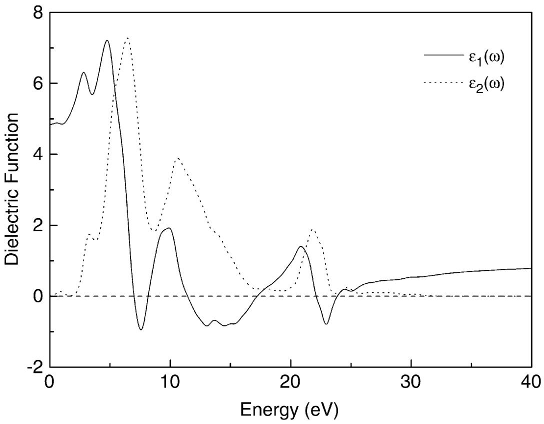

Fig. 8. The imaginary part $\varepsilon_2(\omega)$ and real part $\varepsilon_1(\omega)$ of the dielectric function $\varepsilon(\omega)$ of $CeBr_3$ crystal.

lower intensities for the heights of the peaks. The investigation of the excited state can appropriately explain the origins of absorption peaks. Thus, it is expected to make clear the reasons that lead to the discrepancy through further research on the excited state for $CeCl_3$ in the future. To our knowledge, there have not been yet any experimental results on the dielectric function, refractive index, extinction coefficient and reflectivity. Therefore, we hope that our results could serve as a reference for future experimental study.

Fig. 8 shows the calculated dielectric function of $CeBr_3$. The absorption spectra of $CeBr_3$ are shown in Fig. 6(b). In the Fig. 7(a)–(c), the dashed line shows the calculated results of the refractive index, extinction coefficient and reflectivity of $CeBr_3$, respectively. They exhibit similar features to optical properties of $CeCl_3$.

6. Summary and conclusions

In summary, we calculate the crystal structure, band structure, density of states, and optical properties of $CeCl_3$ and $CeBr_3$ by means of the density functional theory within the generalized gradient approximation. Our structural parameters are in good agreement with the experimental results. The electronic structures and absorption spectra of $CeCl_3$ and $CeBr_3$ are obtained and compared with the experimental data. Our results show good agreement with the available experimental data when we considered the 4f states of Ce as core state. We also present the dielectric function, refractive index, extinction coefficient and reflectivity of $CeCl_3$ and $CeBr_3$. Moreover, the imaginary part $\varepsilon_2(\omega)$ of the dielectric function is discussed in detail. We are not aware of any published data on the dielectric function, refractive index, extinction coefficient and reflectivity of $CeCl_3$ and $CeBr_3$ materials. Therefore, our results can be used to cover this lack of data for $CeCl_3$ and $CeBr_3$.

Acknowledgements

This work was supported by the National Natural Science Foundation of China (10572155, 10172030, 50232030) and The Science Foundation of Guangdong Province (2005A1060-2002).

References

[1] V. Vetere, C. Adamo, P. Maldivi, Chem. Phys. Lett. 325 (2000) 99.
[2] R.D. Wesley, C.W. Dekock, J. Chem. Phys. 55 (1971) 3866.
[3] C.S. Shi, Y.H. Chen, G.B. Zhang, X.L. Xu, H.G. Tang, Chin. J. Lumin. 3 (2002) 218.
[4] C.G. Olson, M. Piacentini, D.W. Lynch, Phys. Rev. B 18 (1978) 5740.
[5] L. Joubert, G. Picard, J.J. Legendre, Inorg. Chem. 37 (1998) 1984.
[6] T. Tsuchiya, T. Taketsugu, H. Nakano, K. Hirao, J. Mol. Struct. (Theochem) 461–462 (1999) 203.
[7] A. Kovacs, R.J.M. Konings, A.S. Booij, Vib. Spectrosc. 10 (1995) 65.
[8] A. Kovacs, J. Mol. Struct. 482–483 (1999) 403.
[9] O.G. Noel, J.T.M. de Haas, P. Dorenbos, C.W.E. van Eijk, K. Kramer, H.U. Gudel, J. Lumin. 85 (1999) 21.
[10] K.S. Shah, J. Glodo, W. Higgins, E.V.D. van Loef, W.W. Moses, IEEE Trans. Nucl. Sci. 52 (2005) 3157.
[11] K.H. Park, S.J. Oh, Phys. Rev. B 48 (1993) 14833.
[12] S. Sato, J. Phys. Soc. Japan 41 (1976) 913.
[13] J.P. Perdew, K. Burke, M. Ernzerhof, Phys. Rev. Lett. 77 (1996) 3865.
[14] C. Adamo, P. Maldivi, J. Phys. Chem. A 102 (1998) 6812.
[15] V. Jonas, W.J. Thiel, J. Chem. Phys. 102 (1995) 8474.
[16] L.A. Eriksson, L.G.M. Pettersson, P.E.M. Siegbahn, U.J. Wahlgren, J. Chem. Phys. 110 (1995) 872.
[17] M. Castro, D.R. Salahub, R. Fournier, J. Chem. Phys. 100 (1994) 8233.
[18] B. Delly, M. Wrinn, H.P. Luthi, J. Chem. Phys. 100 (1994) 5785.
[19] H.J. Monkhorst, J.D. Pack, Phys. Rev. B 13 (1976) 5188.
[20] S. Saha, T.P. Sinha, Phys. Rev. B 62 (2000) 8828.
[21] W.H. Zachariasen, Acta. Crystallogr. 1 (1948) 265.
[22] W.H. Zachariasen, J. Chem. Phys. 16 (1948) 254.
[23] N.V. Skorodumova, R. Ahuja, S.I. Simak, A. Abrikosov, B. Johansson, B.I. Lundqvist, Phys. Rev. B 64 (2001) 115108.
[24] F. Goubin, X. Rocquefelte, D. Pauwels, A. Tressaud, A. Demourgues, S. Jobic, Y. Montardi, J. Solid State Chem. 177 (2004) 2833.
[25] M.Q. Cai, Z. Yin, M.S. Zhang, Appl. Phys. Lett. 83 (2003) 14.
[26] J.S. de Almeida, R. Ahuja, Appl. Phys. Lett. 89 (2006) 061913.
[27] R. Khenata, M. Sahnoun, H. Baltache, M. Rerat, A.H. Rashek, N. Illes, B. Bouhafs, Solid State Commun. 136 (2005) 120.